Reducing Power Consumption of Tilt-Wing eVTOL Aircraft during Hovering Flight in Crosswind

Masatoshi Mizuno* Student Member, Kentaro Yokota* Student Member
Hiroshi Fujimoto* Senior Member

Recently, the number of companies which participate in flying cars such as electric vertical take-off and landing (eVTOL) aircraft has been increasing. Those aircraft are expected as traffic jam relaxation and transportation means in the disaster. However, there are very few examples of practical application because eVTOL aircraft has some problems in cruising range and safety. In this study, we propose a method to reduce the power consumption during hovering. The proposed system achieves power reduction by about 1 %.

Keywords: Tilt-Wing, eVTOL, power optimization

1. Introduction

1.1 Recent flying cars Recently, the number of companies which are active in the development of flying cars such as Airbus in France, Uber Elevate in U.S.A., SkyDrive in Japan, etc. have been increasing. Many of them are scheduled for practical application in 2023. Flying cars are made based on electric vertical take-off and landing (eVTOL) aircraft and they are expected as traffic jam relaxation and transportation means in the disaster. However, few flight tests have been conducted, and there are large problems in the safety. Regarding the cruising range, an eVTOL aircraft has a shorter range than an electric vehicle (EV). In Europe, before commercial flight of an eVTOL aircraft, it must be certified by the civil aviation authority, and proper thrust and energy management are major hurdles [1]. It means the main problems of flying car are stability and cruising range.

Flying cars are often categorized into four types: Multicopter, Tilt-Rotor, Tilt-Wing and a type with Lift + Cruise rotors, of which Tilt-Wing is a efficient type [1]. Considerable efficiency improvements are possible utilizing distributed electric propulsion (DEP) technology because it enables a fixed-wing eVTOL to provide lift with far higher efficiency than rotors especially in cruise phase [2]. In addition, to the improved cruise efficiency a tandem Tilt-Wing has an advantage of lower power consumption in hover than a Tilt-Rotor as the impact of the rotor downwash on the wing is substantially effect [3]. A Tilt-Wing has an additional benefit as the induced airflow behind the rotors reduces the angle of attack on the wing in hover and low-speed forward flight [4].

1.2 Previous studies on Tilt-Wing eVTOL A Tilt-Wing eVTOL flys in the three phases of hovering, transition, and cruise as shown in Figure 1. Since the main wing is easily affected by a disturbance in hovering, the attitude tends to become unstable. Among these disturbances, elevon and tail rotors are effective [5]. Model predictive control (MPC) has been applied to improve the tracking performance in hovering [6]. On the other hand, in a Multicopter, by tilting each rotor, pitching and yawing moment can be efficiently increased to suppress disturbance [7][8]. These are expected to be applied to the Tilt-Wing type in terms of tilting the rotor.

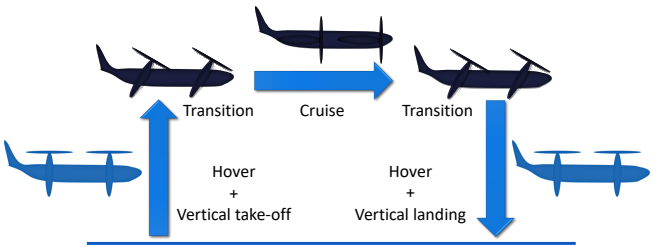

Figure 1. A whole flight of Tilt-Wing eVTOL aircraft.

In the transition, since there are many kinds of aerodynamic changes such as drag or airspeed, tilt angle, rotational speed of rotor, etc. which act on the airframe, it is easy to become unstable, and the research is widely carried out [9]~[13].

Also, there is research on a controller that can be applied to the whole flight to stabilize a Tilt-Wing aircraft regardless of the flight phase [14]~[18]. Especially, in Japan Aerospace Exploration Agency, a controller using stability augmentation system and control augmentation system has been studied [19]~[22].

On the power consumption model necessary for considering the flight range of an eVTOL, the model adaptable to various eVTOL operating at every conditions of vertical take-off and landing, cruise, and transition is studied [1]. Also, in the flight of eVTOL, the power consumption during hovering is the largest [4]. However, Tilt-Wing eVTOL has many problems in stability, so there are few studies on the range extension.

1.3 Necessity and problems of hovering While some form of a structured airspace is capable, it is expected that flying cars will be required to deal with high traffic densities and will need to respond to conflicts due to a dynam-

* The University of Tokyo, 5-1-5, Kashiwanoha, Kashiwa, Chiba, 227-8561 Japan

Table 1. Nomenclature.

Parameter	Definition	Unit
α	angle of attack	deg
ρ	air density	kg/m^3
σ	tilt angle	deg
x, y, z	position of aircraft	m
ϕ, θ, ψ	attitude angles of aircraft	deg
L	lift of wing	N
D	drag of wing	N
M	pitching moment of wing	N m
n	rotational speed of propeller	rps
J	advance ratio	–
J_ω	inertia moment of propeller	kg m^2
D_p	propeller diameter	m
C_F	thrust coefficient of propeller	–
C_Q	torque coefficient of propeller	–
Q	counter torque of propeller	N m
F	thrust of rotor	N
F_G	gravity force	N
P	power of aircraft	W
P_{th}	power of rotor	W
P_m, P_c, P_i	mechanical, copper and iron loss of motor	W
i_{od}, i_{oq}	subtraction of copper loss current to dq-axis current of motor	A
L_d, L_q	d-axis and q-axis inductance of motor	H
R_c, R_i	copper and ilon resistance of motor	Ω
K_t	torque constant	N m/A
m	wight of aircraft	kg
S_a	wing area	m^2
I_{xx}, I_{yy}, I_{zz}	inertia moment of aircraft	kg m^2
l_l	rotor distance to center of gravity along x axis	m
l_s	rotor distance to center of gravity along y axis	m
V	airspeed	m/s

ically changing aerodynamics [23]. It is more efficient to wait on the vertiport until it can arrive, according to the most effective speed profile computation under arrival time-constraint for the operational success of tandem Tilt-Wing eVTOL aircraft [4].

1.4 About this paper In terms of the need for hovering and the reduction of power consumption with Tilt-Wing, we propose a method to reduce the power in hovering. In this paper, Section 2 introduces the system of reducing the power in hovering. Section 3 and 4 introduce each of controllers. Simulation results are shown in Section 5 and experimental results are shown in Section 6.

2. Power optimization system design

Figure 2 shows the system to reduce the power in hovering with Tilt-Wing. It includes Model based feedfoward controller, search system and position and attitude controller. figplot shows the position and attitude controller. The gains of the controller are selected by tuning. Propeller force commands are converted for each propeller thrust.

Tilt angles are optimized by the following operation.

1. Yaw the fuselage to bring the crosswind into a headwind
2. Enter a position command to hover
3. Measure the airspeed in front of the aircraft with a pitot tube
4. Calculate the exploration start point of the tilt angle by Model based feedforward controller
5. Search the tilt angles to reduce power consumption with the search system
6. Control the eVTOL by the position and attitude controller

1–3 can be feasible by prior methods, so 4–6 which is the process that the system searches the tilt angle is explained in this paper.

3. Model based feedforward controller

The balance of forces in each direction of the aircraft in a steady state at the airspeed V are expressed as follows:

$$x_b : -F_G \sin\theta - F \sin\left(\sigma - \frac{\pi}{2}\right) + D = 0, \quad \cdots\cdots (1)$$

$$z_b : F\cos\left(\sigma - \frac{\pi}{2}\right) + L - F_G\cos\theta = 0, \quad \cdots\cdots (2)$$

Pitching moment is expressed as below:

$$M_t = M_{th} + M_w = 0, \quad \cdots\cdots (3)$$

where

$$M_{th} = \sum_{i=1}^{4} F_i l_l \sin\sigma - \sum_{i=4}^{8} F_i l_l \sin\sigma, \quad \cdots\cdots (4)$$

$$M_w = \sum_{i=1}^{2} L_i l_l - \sum_{i=2}^{4} L_i l_l + M. \quad \cdots\cdots (5)$$

At this time, the thrust F and counter torque Q of the propeller of each rotor are expressed by advance ratio J as follows:

$$J = \frac{V\cos\alpha}{nD_p}, \quad \cdots\cdots (6)$$

$$F = C_F(J)\rho n^2 D_p^4, \quad \cdots\cdots (7)$$

$$Q = C_Q(J)\rho n^2 D_p^5. \quad \cdots\cdots (8)$$

Represented by Q, the power of each rotor is given by

$$P_{th} = P_m + P_c + P_i. \quad \cdots\cdots (9)$$

If d-axis current is 0, (9) are written as follows [24]:

$$P_m = 2\pi n Q, \quad \cdots\cdots (10)$$

$$P_c = \frac{R_c}{K_t^2} Q^2, \quad \cdots\cdots (11)$$

$$P_i = \frac{(2\pi n)^2}{Ri}\left\{(L_d i_{od} + K_t)^2 + \left(L_q i_{oq}\right)^2\right\}, \quad \cdots\cdots (12)$$

where

$$i_{od} = \frac{1}{R_i^2 + (2\pi n)^2 L_q L_d}\left\{2\pi n L_q R_i \frac{Q}{K_t} - (2\pi n)^2 L_q K_t\right\}, \quad (13)$$

$$i_{oq} = \frac{1}{R_i^2 + (2\pi n)^2 L_q L_d}\left\{R_i^2\left(\frac{Q}{K_t}\right) - 2\pi n K_t R_i\right\}. \quad \cdots\cdots (14)$$

Since wings are fixed by the worm gear in steady state, the power of the eVTOL is as follows:

$$P = \sum_{i=1}^{8} P_{th_i}. \quad \cdots\cdots (15)$$

It considers the number of rotors as shown in Figure 4. By (1)–(3) and (15), a map of power consumption shown in Figure 5 can be obtained. According to the measured airspeed, an exploration start point of tilt angles is determined based on the map.

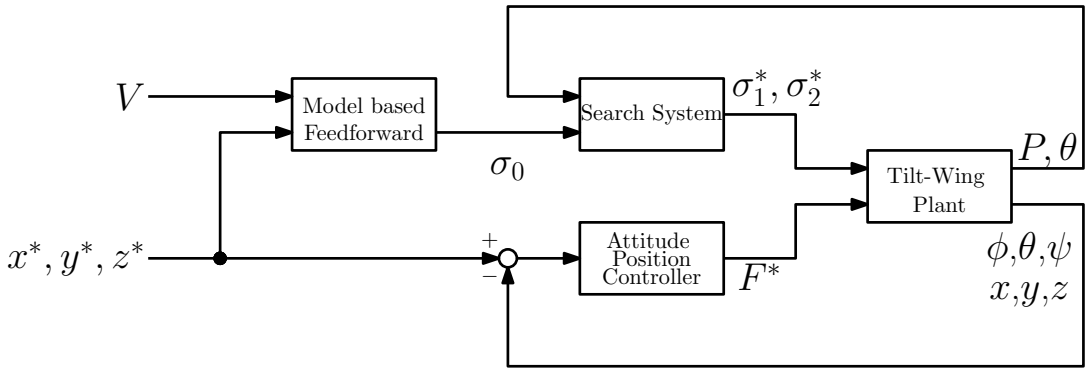

(a) Overall structure.

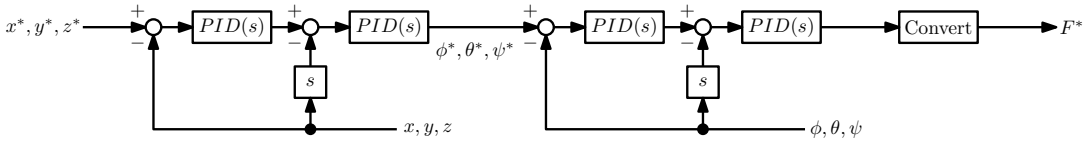

(b) Position and Attitude Controller.

Figure 2. Power optimization system with Tilt-Wing.

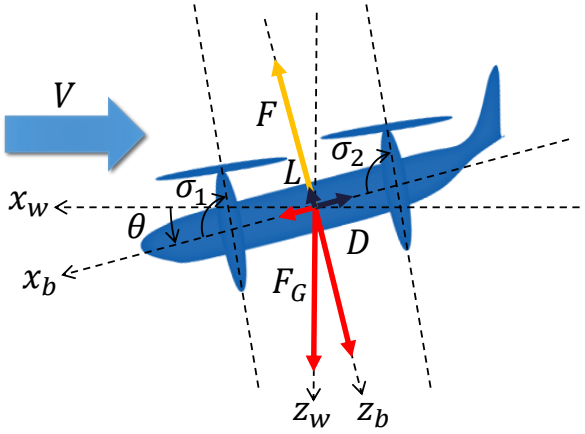

Figure 3. Body dynamics of the Tilt-Wing eVTOL.

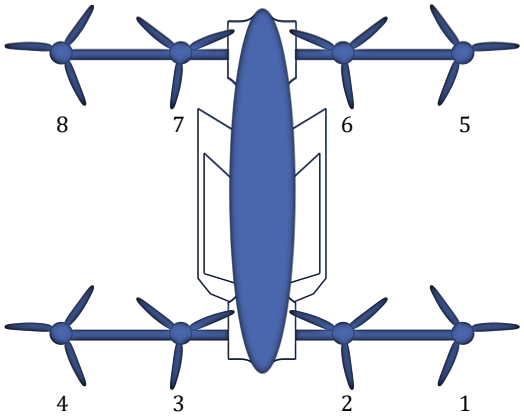

Figure 4. Upper surface of the Tilt-Wing eVTOL with 8 rotors.

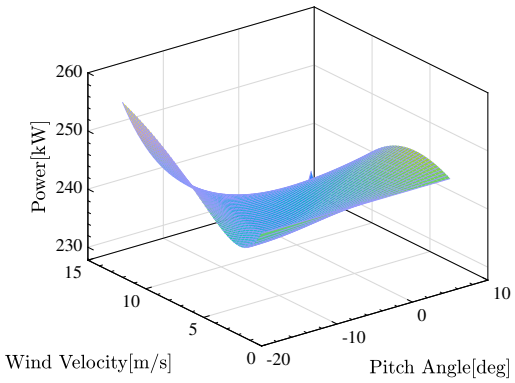

(a) Pitch Angle and Wind Velocity vs. Power.

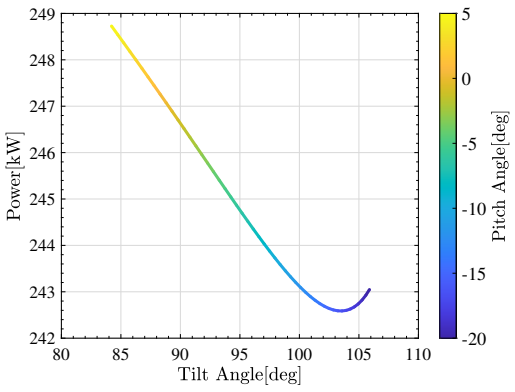

(b) Tilt Angle vs. Power ($V = 2\,\mathrm{m/s}$).

Figure 5. Map for feedforward controller.

4. Tilt angle search system

Steepest descent method is used for the tilt angle search system. Steepest descent method gives a step size of δ and a search direction of s for the single peak performance index $f(x)$,

$$f(x_i + \delta s) - f(x_i) = \left(\frac{\partial f}{\partial x}(x_i)\, s\right)\delta + o(\delta) \cdots\cdots\cdots \quad (16)$$

by updating the step size δ and the search direction s as (16). The optimum point can be obtained by searching until the gradient of the evaluation function becomes appropriately small. The specific procedure is as follows:

Table 2. Specifications of the Tilt-Wing eVTOL.

Parameter	Value
m	726 kg
D_p	1.5 m
S_a	4.5 m^2
I_{xx}	1.07×10^3 kg m^2
I_{yy}	0.74×10^3 kg m^2
I_{zz}	0.74×10^3 kg m^2
l_l	2.0 m
l_s	1.5 m
Rated output of the motor	45 kW
Number of rotors	8

Table 3. Parameters for simulation.

Parameter	Value
V	2 m/s
J_ω	0.55 kg m^2
ρ	1.22 kg/m^3
R_c	0.140 Ω
R_i	0.01 Ω
L_q	48.4 mH
L_d	48.4 mH
K_t	0.361 N m/A

1. Give the start point x_0
2. If $\left|\frac{\partial f}{\partial x}\right|$ is greater than desired, proceed to the next step
3. Culculate and update : $s = -\left(\frac{\partial f}{\partial x}(x_i)\right)^T$
4. Update : $x_{i+1} = x_i + \delta s$

In this controller, the evaluation function is defined as eVTOL's power P, and the state variables are defined as two tilt angles $[\sigma_1, \sigma_2]$. The exploration is performed by feeding back the power P while updating two tilt angles alternately. The step size δ is treated as a constant because the evaluation function P is unknown. The exploration ends when the gradient of P becomes smaller than the minimum step of tilt angle or when the pitch angle θ of the eVTOL tilts to a predetermined limit value.

5. Simulation

In the simulation, parameters of the eVTOL were set as shown in Table 2 referring to Vahana of Airbus [(2)(4)(13)]. The simulation conditions are that the eVTOL is hovering in airspeed of 2 m/s, and the performance of the proposed system is compared with that of a fixed tilt angle of 90 deg.

The simulation results are shown in Figure 6. As shown in Figure 6(d), when the feedforward controller is turned on, tilt angles fluctuates, and then the search system investigated tilt angles to reduce power consumption. At this time, the thrust of each rotor also changed according to the change of the tilt angles. As shown in Figure 6(a) and Figure 6(b), the power decreased by about 1 % compared with the case where the tilt angle was fixed at 90 deg. This is because the thrusts decreased as shown in Figure 6(e) and Figure 6(f). However, as shown in Figure 6(c), as for the position, it deteriorated compared to the fixed tilt angle since the fluctuation of the tilt angles becomes a disturbance.

6. Experiment

In order to show the validity of the aircraft model, an experiment was carried out considering the rotation of a wing and propeller in a large angle of attack.

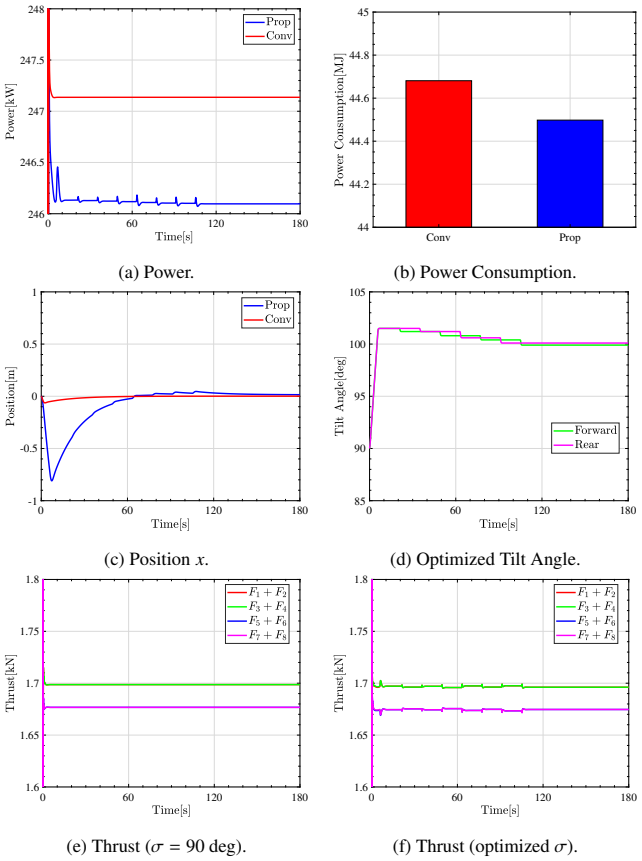

(a) Power. (b) Power Consumption.

(c) Position x. (d) Optimized Tilt Angle.

(e) Thrust (σ = 90 deg). (f) Thrust (optimized σ).

Figure 6. Simulation results for minimizing power in hovering ($V = 2$ m/s).

The experimental apparatus consists of a wing model, an air circulator, and a load cell as shown in Figure 7. The load cell, WDF-6-A-100-2-AC1 manufactured by Wacohtech, can measure the force and moment in each direction separately. The specifications of the wing model used in the experiment are shown in Table 4, and the Clark Y model was adopted for the wing shape.

In the experiment, the characteristics of the lift, drag and thrust against the change of the angle of attack and the power of the motor were measured by making the airspeed and the number of revolutions of the propeller constant value.

The experimental results are shown in Figure 8. Figure 8(a) and Figure 8(b) shows the forces on the wing in each direction, with the x-axis and y-axis corresponding to x_b-axis and z_b-axis of Figure 3. The pitching moment acting on the wing changes similarly as shown in Figure 8(c). The greater the angle of attack, the greater the drag on the wing, and the greater the force moving the fuselage horizontally. On the other hand, when the number of revolutions of the propeller is constant, the amount of air flowing into the propeller changes according to the change in the angle of attack, so that the thrust changes as (9)–(15). Therefore, the power of the rotor depends on the angle of attack as shown in Figure 8(d).

As the experimental results show, power can be reduced by maintaining hovering by tilting the wings with steady crosswind, since lift and power vary depending on the angle of

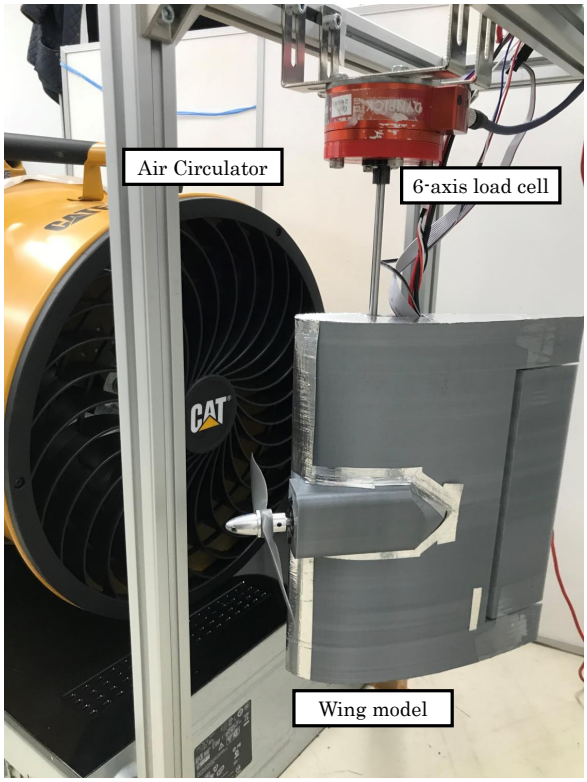

(a) Overall appearance.

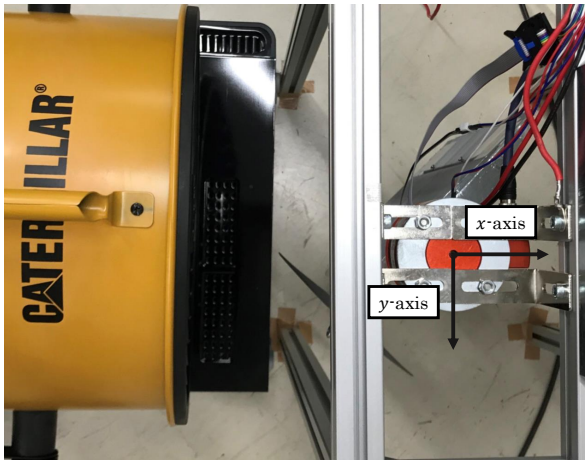

(b) Upper side.

Figure 7. Experimental apparatus for characteristic in a large angle of attack.

Table 4. Specifications of the wing model.

Parameter	Value
wing area	678 cm^2
chord length	23 cm
wingspan	29.5 cm
weight	1.6 kg
propeller diameter	20.32 cm
rated power of the moter	70 W

attack of the wing.

In the future, the relationship between the tilt angle and power consumption will be shown through experiments, and the operation of the proposed control system will be demonstrated.

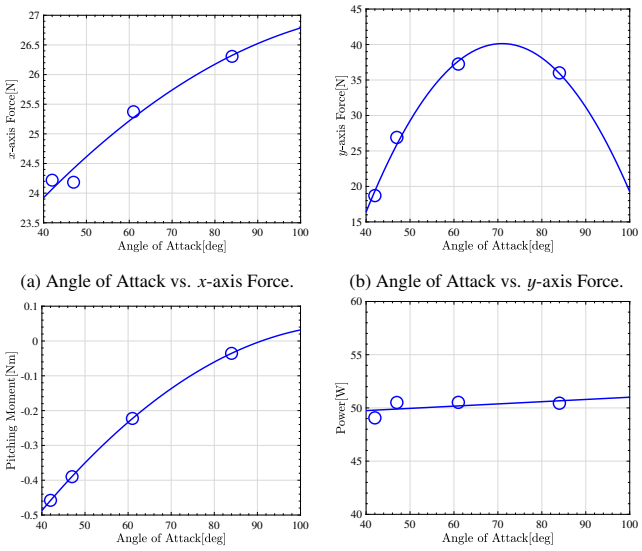

(a) Angle of Attack vs. x-axis Force.

(b) Angle of Attack vs. y-axis Force.

(c) Angle of Attack vs. Pitching Moment.

(d) Angle of Attack vs. Power

Figure 8. Experimental result for characteristic in a large angle of attack with constant propeller speed and airspeed ($V = 4\,\mathrm{m/s}$).

7. Conclusion

In this paper, we propose a method to improve the power consumption during hovering. Flying cars are assumed to be operated at an altitude of 300 m or more, and in such a space, a steady cross wind blows against an airframe by weather conditions. In the proposed method, power consumption in hovering was reduced by moving the tilt angle using such cross wind. The system of the proposed method is as shown in Figure 2, and by compensating the change of the dynamics for the fluctuation of the tilt angle by the position and attitude controller, it is possible to reduce the power consumption while keeping the hovering.

The feedforward controller based on the aircraft model can reduce the calculation cost of the search system and the position and attitude controller, while the starting points are obtained for the tilt angle exploration. In the tilt angle exploration system, it was used in order to deal with modeling error which can not be considered by the feedforward controller . In order to reduce the power consumption, and the exploration using the steepest descent method with small fluctuation of the tilt angle was adopted.

In the simulation, as shown in Figure 6, the power consumption decreases about 1 % than when fixed at 90 deg. However, the position was deteriorated in compared to that of the fixed tilt angle, since the fluctuation of the tilt angles became a disturbance.

In the future, the relationship between the tilt angle and power consumption will be shown through experiments, and the operation of the proposed control system will be demonstrated.

Acknowledgement

This work was partly supported by JSPS KAKENHI Grant Number JP18H03768.

References

(1) E. Senkans, M. Skuhersky, M. Wilde, and B. Kish, "A First-Principle Power and Energy Model for eVTOL Vehicles," in *AIAA Scitech 2020 Forum*, no. January, (Reston, Virginia), pp. 1–22, American Institute of Aeronautics and Astronautics, jan 2020.

(2) "Vahana Configuration Trade Study — Part I." `https://acubed.airbus.com/blog/vahana/vahana-configuration-trade-study-part-i/`, 2016.

(3) K. Muraoka, N. Okada, and D. Kubo, "Quad Tilt Wing VTOL UAV: Aerodynamic Characteristics and Prototype Flight," in *AIAA Infotech@Aerospace Conference*, no. April, (Reston, Virigina), pp. 6–13, American Institute of Aeronautics and Astronautics, apr 2009.

(4) P. Pradeep and P. Wei, "Energy Optimal Speed Profile for Arrival of Tandem Tilt-Wing eVTOL Aircraft with RTA Constraint," in *2018 IEEE CSAA Guidance, Navigation and Control Conference, CGNCC 2018*, 2018.

(5) L. M. Sanchez-Rivera, R. Lozano, and A. Arias-Montano, "Pitching moment analysis and adjustment for tilt-wing UAV in VTOL mode," in *2019 International Conference on Unmanned Aircraft Systems (ICUAS)*, pp. 1445–1450, IEEE, jun 2019.

(6) K. Benkhoud and S. Bouallegue, "Model Predictive Control design for a convertible Quad Tilt-Wing UAV," *4th International Conference on Control Engineering and Information Technology, CEIT 2016*, pp. 16–18, 2017.

(7) C. Holda, B. Ghalamchi, and M. W. Mueller, "Tilting multicopter rotors for increased power efficiency and yaw authority," in *2018 International Conference on Unmanned Aircraft Systems (ICUAS)*, pp. 143–148, IEEE, jun 2018.

(8) H. Otsuka and K. Nagatani, "Reduction of pitching moment generation of a quadrotor UAV in gust with slant rotors," *AIAA SciTech Forum - 55th AIAA Aerospace Sciences Meeting*, no. January, pp. 1–14, 2017.

(9) K. Muraoka, N. Okada, D. Kubo, and M. Daisuk, "Transition flight of quad tilt wing VTOL UAV," *28th Congress of the International Council of the Aeronautical Sciences 2012, ICAS 2012*, vol. 4, pp. 3242–3251, 2012.

(10) D. S. B. Shaiful, L. T. S. Win, J. E. Low, S. K. H. Win, G. S. Soh, and S. Foong, "Optimized transition path of a transformable hovering rotorcraft (THOR)," *IEEE/ASME International Conference on Advanced Intelligent Mechatronics, AIM*, vol. 2018-July, pp. 460–465, 2018.

(11) W. Jian-jian, W. Qi, L. Yang, and L. Zhi-han, "A Sliding Mode Altitude Flight Control for a Class of Tilting Wing Aircraft in Transition Flight Stage," in *2019 Chinese Control Conference (CCC)*, pp. 8177–8181, IEEE, jul 2019.

(12) Y. Wang, Y. Zhou, and C. Lin, "Modeling and control for the mode transition of a novel tilt-wing UAV," *Aerospace Science and Technology*, vol. 91, pp. 593–606, 2019.

(13) S. S. Chauhan and J. R. Martins, "Tilt-wing eVTOL takeoff trajectory optimization," *Journal of Aircraft*, vol. 57, no. 1, pp. 93–112, 2020.

(14) E. Small, E. Fresk, G. Andrikopoulos, and G. Nikolakopoulos, "Modelling and control of a Tilt-Wing Unmanned Aerial Vehicle," *24th Mediterranean Conference on Control and Automation, MED 2016*, pp. 1254–1259, 2016.

(15) K. Benkhoud and S. Bouallègue, "Dynamics modeling and advanced metaheuristics based LQG controller design for a Quad Tilt Wing UAV," *International Journal of Dynamics and Control*, vol. 6, no. 2, pp. 630–651, 2018.

(16) K. Masuda and K. Uchiyama, "Robust control design for Quad Tilt-Wing UAV," *Aerospace*, vol. 5, no. 1, 2018.

(17) F. Binz, T. Islam, and D. Moormann, "Attitude control of tiltwing aircraft using a wing-fixed coordinate system and incremental nonlinear dynamic inversion," *International Journal of Micro Air Vehicles*, vol. 11, pp. 1–12, jan 2019.

(18) D. Rohr, T. Stastny, S. Verling, and R. Siegwart, "Attitude and Cruise Control of a VTOL Tiltwing UAV," *IEEE Robotics and Automation Letters*, vol. 4, no. 3, 2019.

(19) M. SATO and K. MURAOKA, "Flight Control of Quad Tilt Wing Unmanned Aerial Vehicle," *Journal of the Japan Society for Aeronautical and Space Sciences*, vol. 61, no. 4, pp. 110–118, 2013.

(20) M. Sato and K. Muraoka, "Flight controller design and demonstration of quad-tilt-wing unmanned aerial vehicle," *Journal of guidance, control, and dynamics*, vol. 38, no. 6, pp. 1071–1082, 2015.

(21) A. T. Tran, N. Sakamoto, M. Sato, and K. Muraoka, "Control Augmentation System Design for Quad-Tilt-Wing Unmanned Aerial Vehicle via Robust Output Regulation Method," *IEEE Transactions on Aerospace and Electronic Systems*, vol. 53, no. 1, pp. 357–369, 2017.

(22) S. Panza, M. Sato, M. Lovera, and K. Muraoka, "Robust Attitude Control Design of Quad-Tilt-Wing UAV: A Structured μ-Synthesis Approach," *2018 IEEE Conference on Control Technology and Applications, CCTA 2018*, pp. 781–786, 2018.

(23) J. Bertram and P. Wei, "An Efficient Algorithm for Self-Organized Terminal Arrival in Urban Air Mobility," in *AIAA Scitech 2020 Forum*, pp. 1–10, American Institute of Aeronautics and Astronautics, jan 2020.

(24) H. Fujimoto and S. Harada, "Model-based range extension control system for electric vehicles with front and rear driving–braking force distributions," *IEEE Transactions on Industrial Electronics*, vol. 62, no. 5, pp. 3245–3254, 2015.